Electronic Supplementary Material (ESI) for Journal of Materials Chemistry A.

Electronic Supporting Information

Self-Descaling Janus Nanofibrous Evaporator Enabled by A "Moving Interface" for Durable Solar-Driven Desalination of Hypersaline Water

Hao-Nan Li[a,b], Hao-Cheng Yang[c]*, Cheng-Ye Zhu[a,b], Jian Wu[d], Andreas Greiner[e]*, Zhi-Kang Xu[a,b]*

[a] MOE Key Laboratory of Macromolecular Synthesis and Functionalization, and Key Laboratory of Adsorption and Separation Materials & Technologies of Zhejiang Province, Department of Polymer Science and Engineering, Zhejiang University, Hangzhou, 310027, China

[b] The "Belt and Road" Sino-Portugal Joint Lab on Advanced Materials, International Research Center for X Polymers, Zhejiang University, Hangzhou, 310027, China

[c] School of Chemical Engineering and Technology, Sun Yat-Sen University, Southern Marine Science and Engineering Guangdong Laboratory (Zhuhai), No.2 Daxue road, Tangjiawan, Zhuhai 519082, China

[d] Department of Chemistry, Zhejiang University, Hangzhou, 310027, China

[e] Macromolecular Chemistry and Bavarian Polymer Institute, University of Bayreuth, Universitatsstrasse 30, Bayreuth 95440, German

* Correspondence author:

E-mail addresses: yanghch8@mail.sysu.edu.cn (H.-C. Yang)

greiner@uni-bayreuth.de (A. Greiner)

xuzk@zju.edu.cn (Z.-K. Xu)

Results and discussion

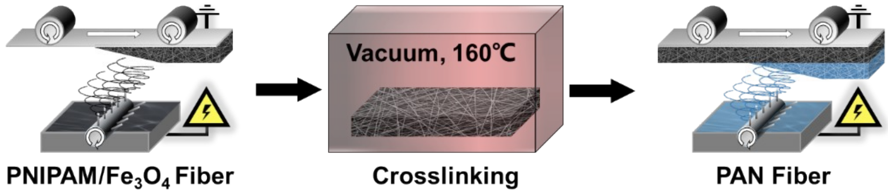

Fig. S1 Schematic diagram of the fabrication process of SJE.

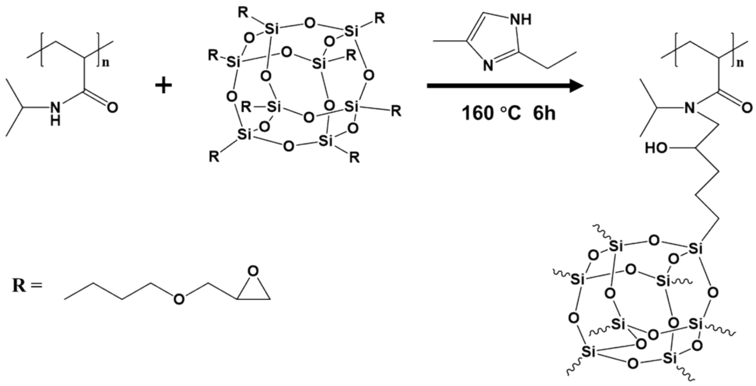

Fig. S2 Scheme of crosslinking reaction of PNIPAM and POSS at 160 ^{o}C.

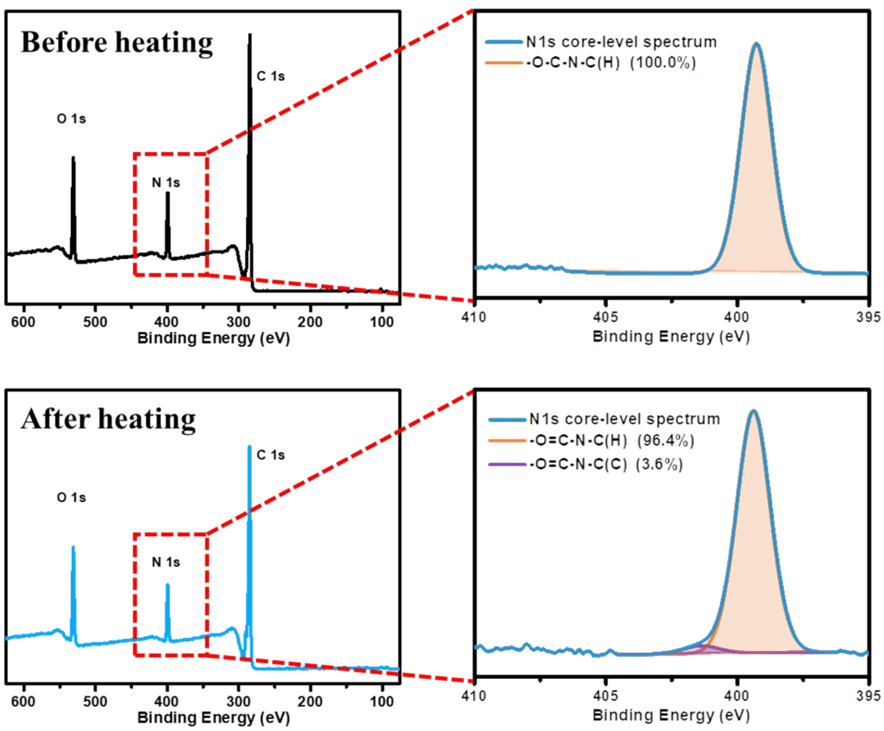

Fig. S3 XPS survey spectra and N 1s core-level spectra of PNIPAM/Fe_3O_4 layers before and after the heating process.

The N 1s core-level spectra of the PNIPAM/Fe_3O_4 layers exhibit a newly-emerged peak located at 401.3 eV after the heating process, which is attributed to O=C–N–C(C) groups of cross-linked PNIPAM. In addition, the main characteristic peak at 399.3 eV belongs to O=C–N–C(H) groups of PNIPAM.[1] Based on the peak area, it can be calculated that there are 3.6% of the repeating units of PNIPAM participated in the cross-linking reaction.

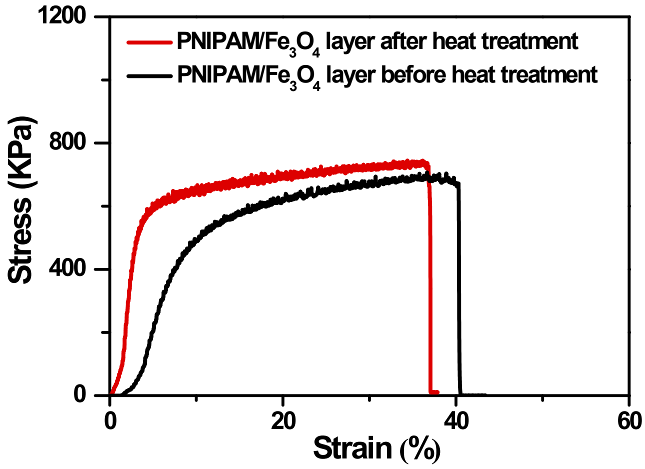

Fig. S4 Stress–strain curves of the PNIPAM/Fe_3O_4 layer before and after heat treatment.

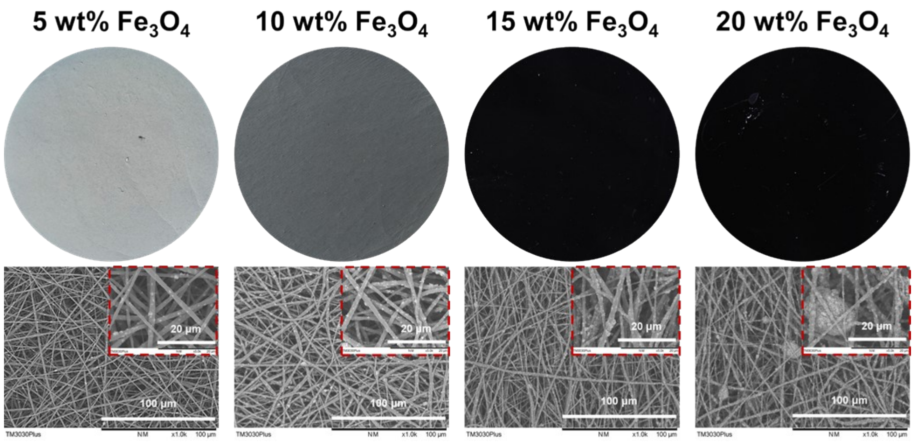

Fig. S5 Digital images (up) and SEM images (down) of the PNIPAM/Fe_3O_4 nanofibrous membrane with different Fe_3O_4 amounts.

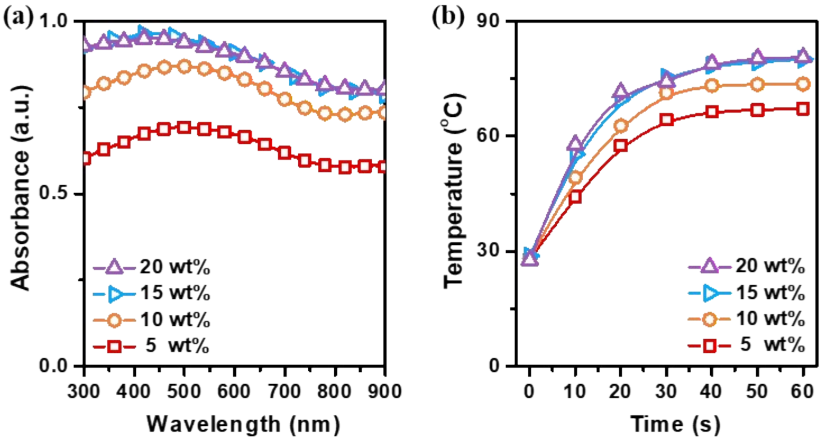

Fig. S6 (a) Light absorption spectra and (b) temperature elevation curves of the PNIPAM/Fe_3O_4 nanofibrous membrane with different Fe_3O_4 amounts.

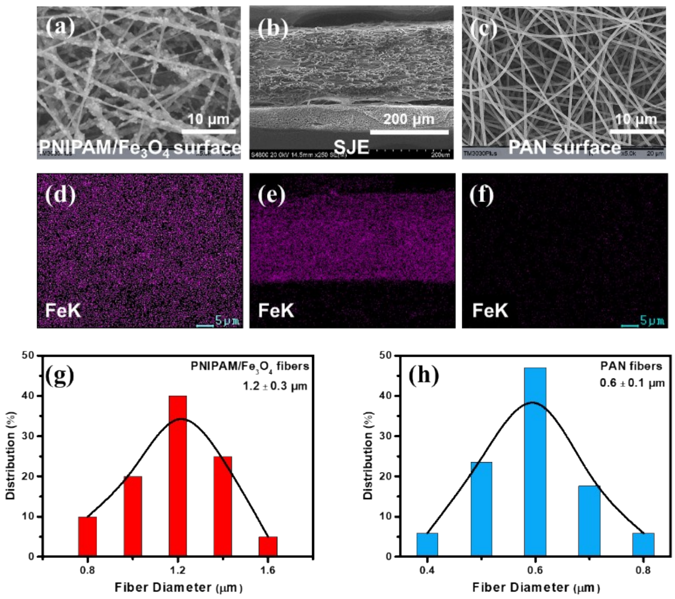

Fig. S7 SEM images of (a) PNIPAM/Fe_3O_4 surface, (b) cross-section and (c) PAN surface of SJEs and corresponding EDX element mapping of Fe of (d) PNIPAM/Fe_3O_4 surface, (e) cross-section and (f) PAN surface. Average fiber diameter distribution of (g) PNIPAM/Fe_3O_4 fibers and (h) PAN fibers.

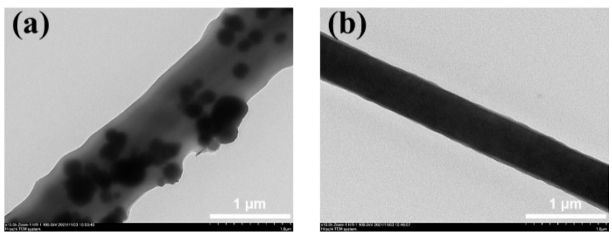

Fig. S8 TEM images of (a) PNIPAM/Fe_3O_4 fibers, (b) PAN fibers. The PNIPAM/ Fe_3O_4 fibers with micro-structured roughness can enhance the multi-scattering of incident light, which is beneficial to improve the light absorption of evaporators.

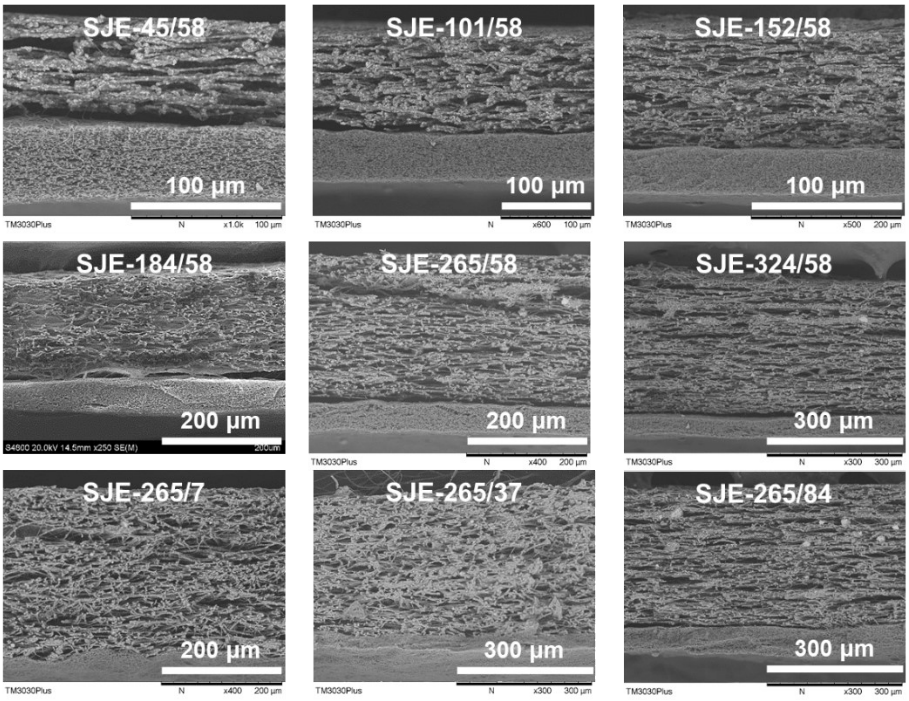

Fig. S9 Corss-section images of SJE.

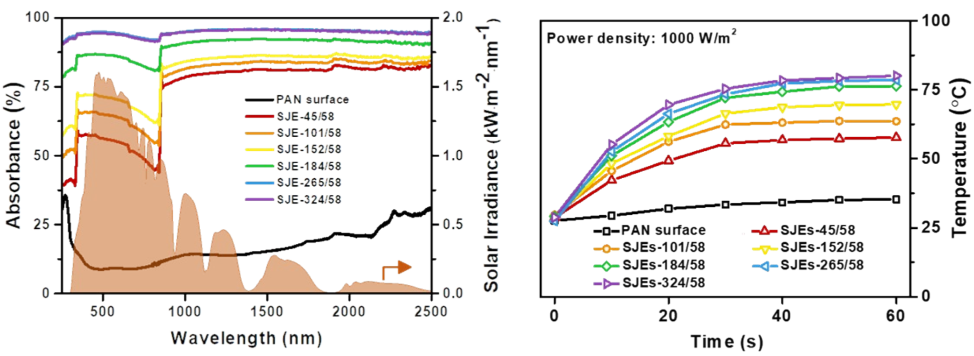

Fig. S10 Full-wave band absorption spectra (left) and dynamic temperature curves (right) of the two surfaces of SJE as a function of time under simulated sunlight irradiation (1000 W/m^2).

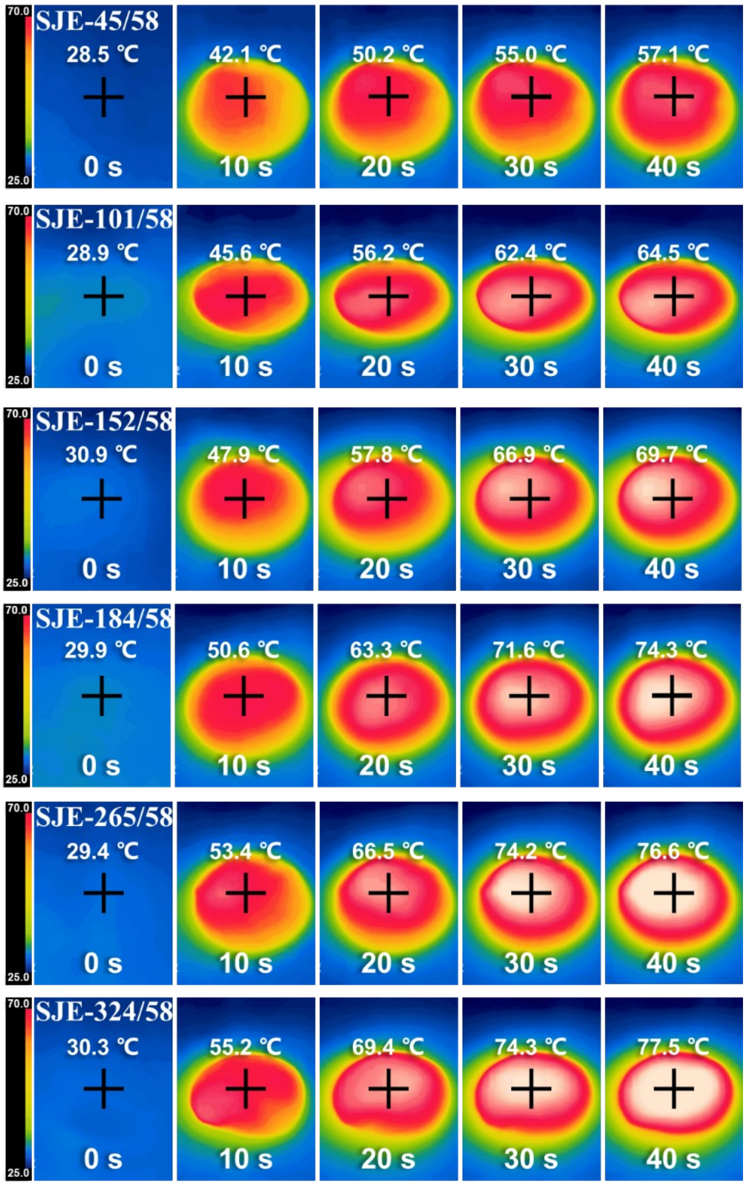

Fig. S11 Infrared images of the PNIPAM/Fe_3O_4 surface of SJE under 1-sun irradiation.

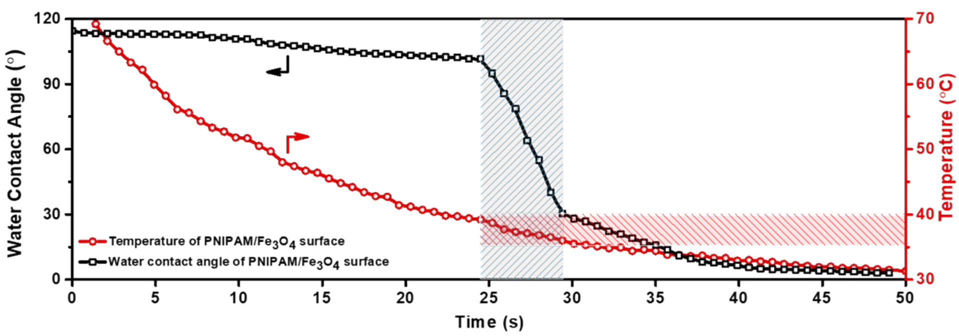

Fig. S12 Dynamic surface temperature and corresponding water contact angle of the PNIPAM/Fe_3O_4 surface of SJE-265/58 during cooling process.

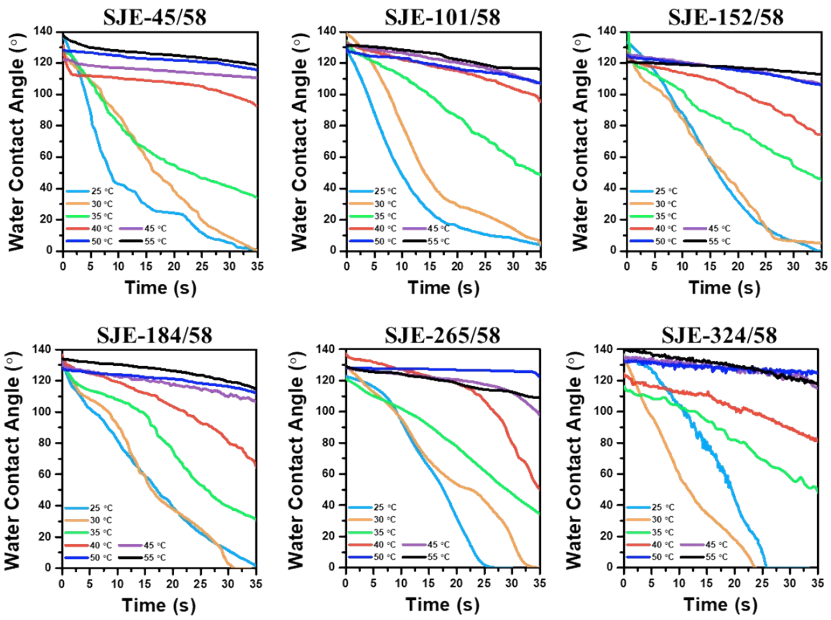

Fig. S13 Dynamic water contact angle of the PNIPAM/Fe_3O_4 surface of SJEs under different temperature.

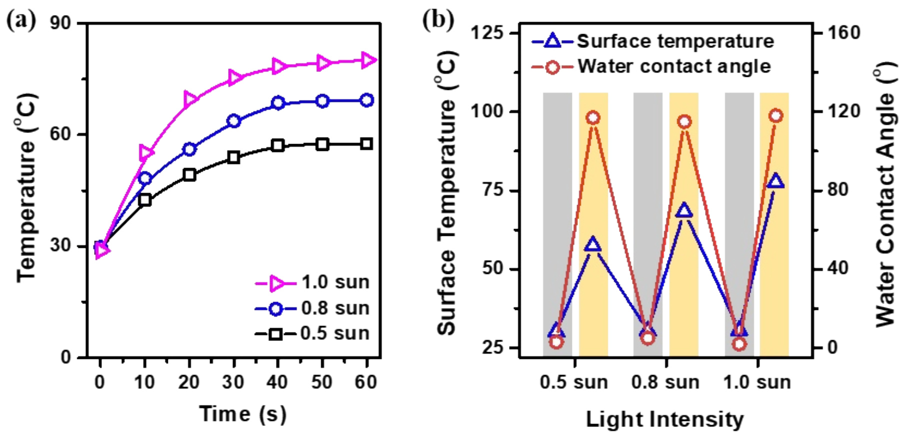

Fig. S14 (a) Temperature elevation curves of the PNIPAM/Fe_3O_4 surface of SJE with the light intensity (0.5 sun, 0.8 sun and 1.0 sun). (b) Static contact angle and surface temperature on the PNIPAM/Fe_3O_4 surface of SJE at different light conditions.

Table S1 Water contact angle (WCA) and surface temperature of the PNIPAM/Fe_3O_4 surface during 100 light-on/light-off cycles.

Cycle Number	Light Condition	Temperature (^{o}C)	WCA (°)
1	off	26	6
	on	75	115
2	off	31	4
	on	78	111
3	off	30	8

	on	77	114
4	off	30	7
	on	78	116
5	off	29	6
	on	74	112
6	off	31	4
	on	76	117
7	off	30	6
	on	77	114
8	off	31	6
	on	72	116
9	off	30	5
	on	74	113
10	off	31	9
	on	76	111
11	off	30	8
	on	76	114
12	off	31	6
	on	78	114
13	off	30	8
	on	76	116
14	off	29	8
	on	77	113
15	off	29	11
	on	74	109
16	off	30	7
	on	73	117
17	off	31	5
	on	78	114
18	off	29	7
	on	77	111
19	off	31	4
	on	73	117
20	off	32	7
	on	76	114
21	off	30	8
	on	74	113
22	off	31	5
	on	77	115
23	off	32	3
	on	78	117
24	off	31	6
	on	74	111
25	off	30	3
	on	76	112
26	off	31	6
	on	77	114

27	off	31	8
	on	75	113
28	off	32	5
	on	74	111
29	off	31	7
	on	76	116
30	off	31	7
	on	77	111
31	off	30	5
	on	78	113
32	off	31	7
	on	73	114
33	off	30	0
	on	77	112
34	off	30	2
	on	78	115
35	off	29	3
	on	75	118
36	off	31	0
	on	74	116
37	off	31	5
	on	77	114
38	off	31	7
	on	75	111
39	off	30	2
	on	76	117
40	off	31	8
	on	77	109
41	off	30	2
	on	75	117
42	off	31	4
	on	77	114
43	off	31	1
	on	74	117
44	off	30	0
	on	77	112
45	off	31	5
	on	74	114
46	off	30	8
	on	77	116
47	off	31	4
	on	75	115
48	off	30	3
	on	77	117
49	off	31	8
	on	75	112
50	off	30	3

	on	76	112
51	off	31	4
	on	77	115
52	off	31	2
	on	76	111
53	off	30	7
	on	74	115
54	off	30	1
	on	77	116
55	off	30	7
	on	76	116
56	off	30	4
	on	76	117
57	off	31	0
	on	76	116
58	off	31	7
	on	74	112
59	off	31	3
	on	77	115
60	off	31	5
	on	75	118
61	off	31	7
	on	76	111
62	off	31	2
	on	74	114
63	off	31	0
	on	77	112
64	off	31	5
	on	73	113
65	off	30	10
	on	75	113
66	off	30	6
	on	74	114
67	off	31	3
	on	77	112
68	off	30	0
	on	78	111
69	off	31	7
	on	76	118
70	off	31	6
	on	77	115
71	off	30	2
	on	76	117
72	off	31	0
	on	74	111
73	off	31	5
	on	78	113

74	off	30	8
	on	77	119
75	off	31	3
	on	73	108
76	off	31	4
	on	78	115
77	off	31	3
	on	72	116
78	off	31	0
	on	74	117
79	off	29	4
	on	71	116
80	off	30	7
	on	71	113
81	off	29	3
	on	74	112
82	off	28	7
	on	73	114
83	off	30	3
	on	73	118
84	off	30	1
	on	71	119
85	off	29	6
	on	76	117
86	off	30	6
	on	73	113
87	off	31	0
	on	77	116
88	off	29	3
	on	74	117
89	off	30	5
	on	76	114
90	off	31	11
	on	73	118
91	off	30	4
	on	78	112
92	off	29	7
	on	73	116
93	off	31	0
	on	78	113
94	off	30	6
	on	77	111
95	off	29	8
	on	74	116
96	off	31	6
	on	76	113
97	off	32	7

	on	77	111
98	off	31	9
	on	74	114
99	off	34	4
	on	77	112
100	off	30	12
	on	72	114

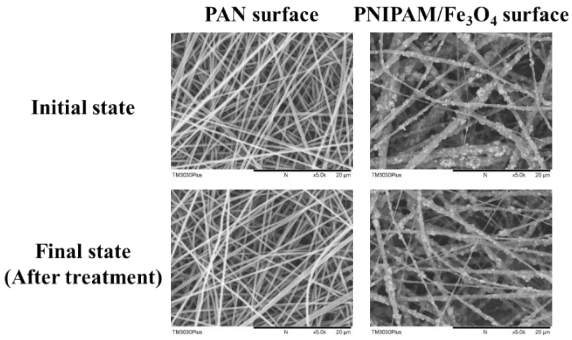

Fig. S15 SEM images of the PAN surface and the PNIPAM/Fe_3O_4 surface of SJE-265/58 before and after cycling test.

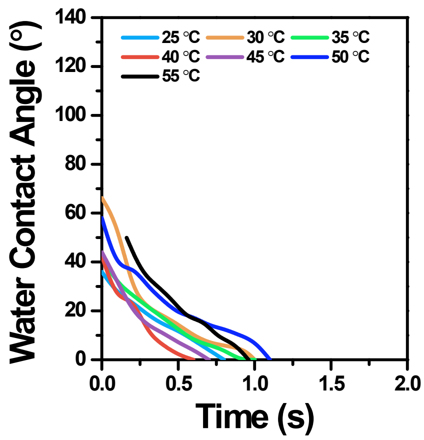

Fig. S16 Dynamic water contact angle of the PAN surface of SJE-265/58 under different temperature.

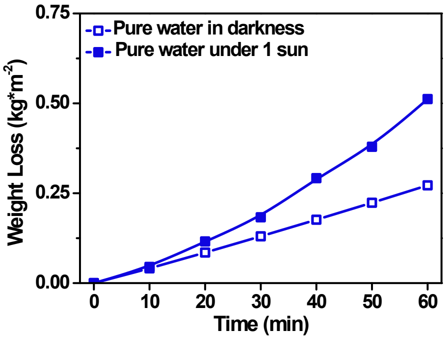

Fig. S17 Mass loss of water over time without SJE under different light conditions.

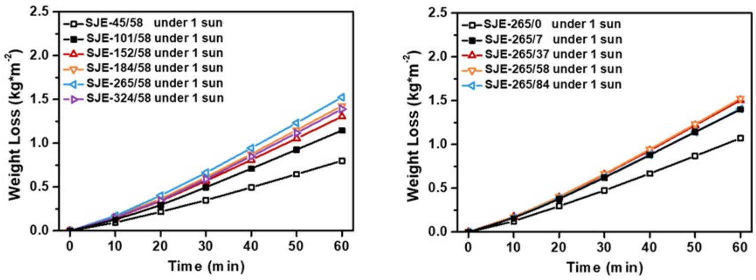

Fig. S18 Mass loss of water over time using different SJEs under 1-sun irradiation.

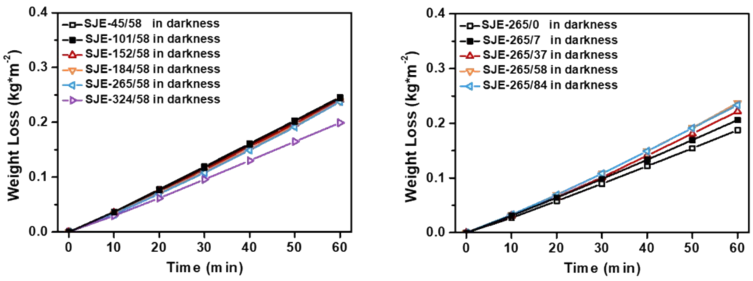

Fig. S19 Mass loss of water over time using different SJEs in darkness.

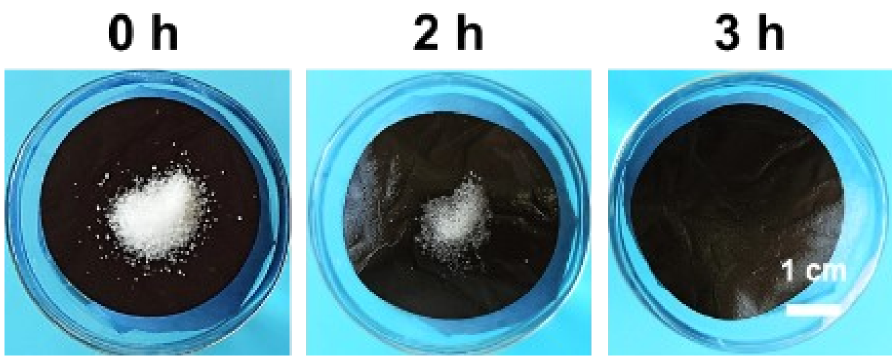

Fig. S20 Photographs showing the capability of self-descaling property by adding 1.5 g NaCl salt on the top surface of SJE.

Table S2 Conductivity of NaCl solution with different NaCl concentration and collected condensed water. The desalination experiments were conducted using the optimized SJE under 1-sun irradiation.

NaCl concentration	Feed ($\cdot 10^3$ μS/cm)	Condensed water (μS/cm)
3.5 wt%	55.4 ± 2.1	12.3 ± 0.5
10.0 wt%	135.2 ± 3.6	11.7 ± 0.8
15.0 wt%	182.1 ± 5.2	13.6 ± 1.1
20.0 wt%	217.4 ± 7.2	12.7 ± 1.8
25.0 wt%	246.3 ± 9.3	14.8 ± 1.1

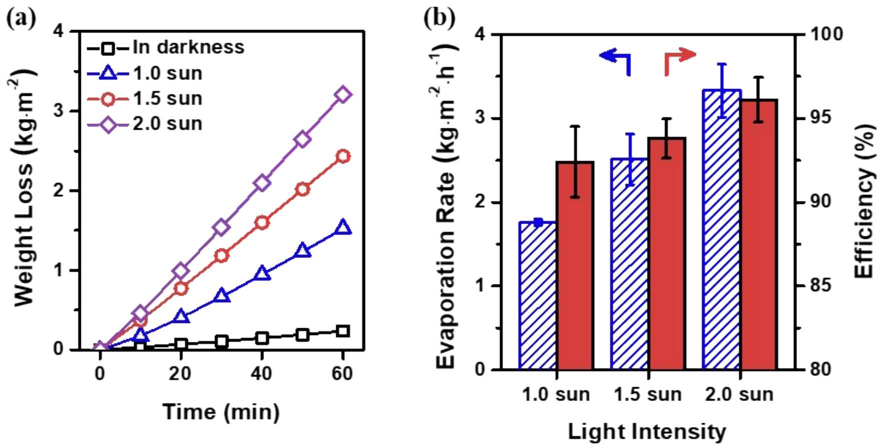

Fig. S21 (a) Mass loss curves, (b) water evaporation rate and corresponding efficiency of SJE under different solar intensity.

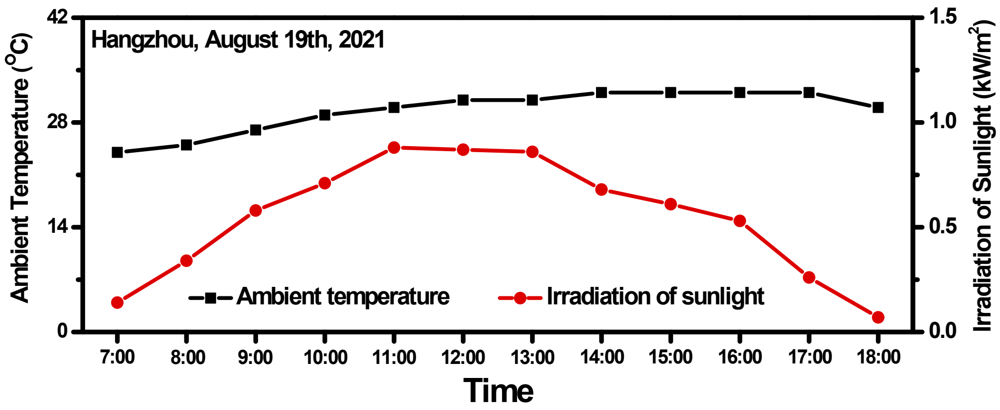

Fig. S22 Ambient temperature and irradiation of sunlight at different times in the actual outdoor experiment.

Table S3 Evaporation rates ($kg{\cdot}m^{-2}{\cdot}h^{-1}$) of different evaporators under1-sun irradiation reported in the literatures

Materials	NaCl concentration in brine (wt%)					Reference
	3.5	10	15	20	25	
Soot-coated Janus evaporator	1.31	/	/	1.28	/	2
Hydroxyapatite nanowires/carbon nanotubes photothermal paper	1.09	/	/	/	/	3
Janus vertically oriented porous membrane	1.58	/	/	/	0.82	4
Laser induced graphene/oxidized laser induced graphene Janus membrane	1.51	/	/	/	/	5
Janus evaporator with low tortuosity pore structure	1.24	1.22	1.21	/	/	6
Vertically aligned Janus MXene aerogel	1.46	1.41	1.44	1.42	/	7
Copper-zinc-tin-selenide assembled membrane	1.53	/	/	/	/	8

Hydrophilic/hydrophobic nanoporous double layer evaporator	1.66	/	/	/	/	9
Janus evaporator with self-recovering surface hydrophobicity	1.38	1.35	/	/	/	10
$W_{18}O_{49}$@PDMS mesocrystal membrane	1.15	/	/	/	/	11
Si/PPy-PVA sponge	1.41	/	/	/	1.35	12
Hierarchical Porous SWCNT Stringed Carbon Polyhedrons and PSS Threaded MOF Bilayer Membrane	1.38	/	/	/	/	13
SWNT/AuNR Janus evaporator	1.85	/	/	/	/	14
PVDF-ATO/PAN nanofiber membrane	0.93	/	/	/	/	15
PDMS/MWCNT/PVDF composite membrane	0.65	/	/	/	/	16
PVDF-HFP Janus evaporator	1.29	/	/	/	/	17
Fe_3O_4/PVDF-HFP photothermal membrane	0.97	/	/	/	1.1	18
SJE	**1.71**	**1.64**	**1.54**	**1.49**	**1.44**	**This work**

References

1 J. Wang, A. Sutti, X. Wang and T. Lin, *Soft Matter*, 2011, **7**, 4364.
2 G. Li, W.-C. Law and K. C. Chan, *Green Chem.*, 2018, **20**, 3689–3695.
3 F. Peng, J. Xu, X. Bai, G. Feng, X. Zeng, M. R. I. Raihan and H. Bao, *Sol. Energ. Mat. Sol. C.*, 2021, **221**, 110910.
4 Z.-C. Xiong, Y.-J. Zhu, D.-D. Qin, F.-F. Chen and R.-L. Yang, *Small*, 2018, **14**, 1803387.
5 H.-H. Yu , L.-J. Yan , Y.-C. Shen, S.-Y. Chen , H.-N. Li, J. Yang and Z.-K. Xu, *Research*, 2020, **2020**, 3241758.
6 D.-D. Han, Z.-D. Chen, J.-C. Li, J.-W. Mao, Z.-Z. Jiao, W. Wang, W. Zhang, Y.-L. Zhang, and H.-B. Sun, *ACS Appl. Mater. Interfaces*, 2020, **12**, 25435−25443.
7 R. Hu, J. Zhang, Y. Kuang, K. Wang, X. Cai, Z. Fang, W. Huang, G. Chen and Z. Wang, *J. Mater. Chem. A*, 2019, **7**, 15333–15340.
8 Q. Zhang, G. Yi, Z. Fu, H. Yu, S. Chen and X. Quan, *ACS Nano*, 2019, **13**, 13196−13207.
9 Y. Yang, W. Que, J. Zhao, Y. Han, M. Ju and X. Yin, *Chem. Eng. J.*, 2019, **373**, 955–962.
10 Y. Yang, H. Zhao, Z. Yin, J. Zhao, X. Yin, N. Li, D. Yin, Y. Li, B. Lei, Y. Du and W. Que, *Mater.*

Horiz., 2018, **5**, 1143-1150.
11 J. Chen, J. L. Yin, B. Li, Z. Ye, D. Liu, D. Ding, F. Qian, N. V. Myung, Q. Zhang, and Y. Yin, *ACS Nano*, 2020, **14**, 17419−17427.
12 Y. Chang, Z. Wang, Y.-e Shi, X. Ma, L. Ma, Y. Zhang and J. Zhan, *J. Mater. Chem. A*, 2018, **6**, 10939–10946.
13 S. Cheng, Z. Yu, Z. Lin, L. Li, Y. Li and Z. Mao, *Chem. Eng. J.*, 2020, **401**, 126108.
14 X. Ma, W. Fang, Y. Guo, Z. Li, D. Chen, W. Ying, Z. Xu, C. Gao and X. Peng, *Small*, 2019, **15**, 1900354.
15 Y. Yang, X. Yang, L. Fu, M. Zou, A. Cao, Y. Du, Q. Yuan and C.-H. Yan, *ACS Energy Lett.*, 2018, **3**, 1165−1171.
16 J. Zhao, Q. Huang, S. Ga, H. Piao, Q. Quan and C. Xiao, *J. Membr. Sci.*, 2021, **635**, 119500.
17 J. Huang, Y. Hu, Y. Bai, Y. He and J. Zhu, *Energy*, 2020, **211**, 118720.
18 W. Li, L. Deng, H. Huang, J. Zhou, Y. Liao, L. Qiu, H. Yang and L. Yao, *ACS Appl. Mater. Interfaces*, 2021, **13**, 26861–26869.